Molecular Devices

# An Electrochemically Controlled Molecular Shuttle**

*Bohdan Korybut-Daszkiewicz,**
*Agnieszka Więckowska, Renata Bilewicz,**
*Sławomir Domagała, and Krzysztof Woźniak**

The design of molecular machines that form assemblies with signal-triggered functions remains a challenging area of research.[1–22] Rotaxanes that contain cyclodextrins, tetrathiafulvalene, porphyrins, or other macrocyclic movable units have been described.[1–4,7–10] The motion between two terminal "stations" in the molecule may result from changes of oxidation state, and thus can be "switched on" by the application of an appropriate potential or laser pulse.[11–15] Catenanes, described by Stoddart and co-workers, almost always contain paraquat as one of the components that has π-acceptor properties.[5,16–19] As a result of π–π interactions, the internal motion of the components may be detected; it can also be switched on chemically owing to the presence of an added species that interacts with one of the components.[20,21] On the other hand, the change of oxidation state of the metal cation component of the catenate induces the movement of the interlocked ring, as demonstrated by Sauvage and co-workers.[22]

Herein we present the first heterodinuclear bismacrocyclic transition-metal complex that exhibits potential-driven intramolecular motion of the interlocked crown-ether unit. Recently, we have demonstrated that the interlocking of the dibenzocrown ether with homo-dinuclear bismacrocyclic transition-metal complexes leads to increased stability of the mixed-valence states, which was reflected in the higher values of conproportionation constants.[23] The observed effect was larger for the dinickel ($d^8$–$d^8$) than for the dicopper ($d^9$–$d^9$) catenane. The interlocked crown ether unit adopts the *cis* conformation in such a manner that one of its aromatic rings is parallel to and between the two metal-coordinating macrocyclic rings. Since both of the coordinated ions were identical, the translocation of the crown-ether moiety from one site to the other produces the same catenane arrangement. However, the intertwining of dibenzo[24]crown-8 with a heterodinuclear bismacrocyclic complex may lead to two possible arrangements, in which the π-electron-rich benzene rings are located in the vicinity of either the copper- or nickel-complexing macrocycle, depending on the oxidation state of the coordinated ions.

The development of appropriate physical methods useful for monitoring the dynamics of supramolecular systems is currently of great importance. Electrochemical methods are especially convenient for monitoring subtle changes in redox properties of electroactive centers, thus reflecting their inter- or intramolecular interactions. Anelli and co-workers demonstrated that bisparaquat cyclophane in [2]catenane is reduced at more negative potentials when interlocked with benzocrown molecules.[1] Electrochemically triggered molecular movement was shown in the case of rotaxanes by Stoddart and co-workers.[24,25] Molecular square schemes illustrating the response of catenates—that is, changes of the coordination geometry—to an electrochemical signal were proposed by Sauvage and co-workers.[26]

Our aim was to synthesize a transition-metal heterodinuclear catenane that should allow a controlled translocation of the crown unit back and forth between two different metal centers in response to an external stimuli, specifically, a potential applied to the electrode.

The synthetic strategy applied to obtain face-to-face hetero-dinuclear bis-macrocyclic complexes (Scheme 1) was different than that described previously for the homo-dinuclear systems.[23] In the first step, the copper(II) coordinated macrocycle was functionalized with two pendant

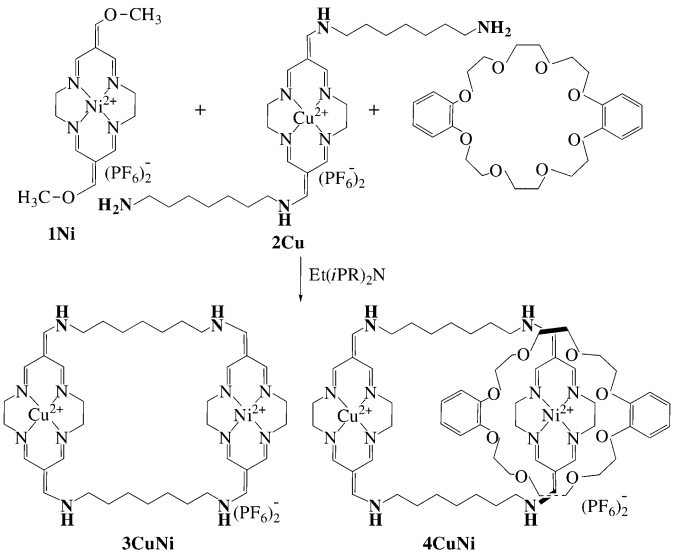


***Scheme 1.*** Synthesis of a heteronuclear [2]catenane.

[*] Dr. habil. B. Korybut-Daszkiewicz
Institute of Organic Chemistry
Polish Academy of Sciences
Kasprzaka 44/52, Warszawa 01-224 (Poland)
Fax: (+48) 226-326-681
E-mail: bkd@icho.edu.pl
Dr. A. Więckowska, Prof. R. Bilewicz
Chemistry Department
Warsaw University
Pasteura 1, 02-093 Warszawa (Poland)
Fax: (+48) 228-220-211/345
E-mail: bilewicz@chem.uw.edu.pl
S. Domagała, Prof. K. Woźniak
Chemistry Department
Warsaw University
Pasteura 1, 02-093 Warszawa (Poland)
Fax: (+48) 228-222-892
E-mail: kwozniak@chem.uw.edu.pl

[**] This work was financially supported by the State Committee for Scientific Research (Project 4 T09A 048 23, 4 T09A 109 22). The X-ray measurements were undertaken in the Crystallographic Unit of the Physical Chemistry Laboratory at the Chemistry Department of the University of Warsaw.

Supporting information for this article is available on the WWW under http://www.angewandte.org or from the author.

 © 2004 Wiley-VCH Verlag GmbH & Co. KGaA, Weinheim DOI: 10.1002/ange.200352528 

diamino linkers to give **2Cu**,[27] which was then cyclized by using the second macrocyclic unit that contained a coordinated nickel(II) ion (**1Ni**). In the presence of an excess of dibenzo[24]crown-8, the hetero-dinuclear bis-macrocycle (**3CuNi**) and catenane (**4CuNi**) were formed with 33% and 12% yields, respectively. The compounds were unambiguously identified by ESI mass spectrometry and characterized by spectroscopic and analytical methods (see Supporting Information).

Compound **4CuNi** crystallizes in the triclinic $P\bar{1}$ space group[28] with one molecule in the independent part of the unit cell. The bis-macrocyclic ring is positively charged because of the presence of $Ni^{II}$ and $Cu^{II}$ ions and the interlocked rings are surrounded by four $PF_6^-$ anions. The crown ether and the large bis-azamacrocyclic ring in **4CuNi** form a sandwichlike structure (Figure 1) in such a way that one of the crown ether

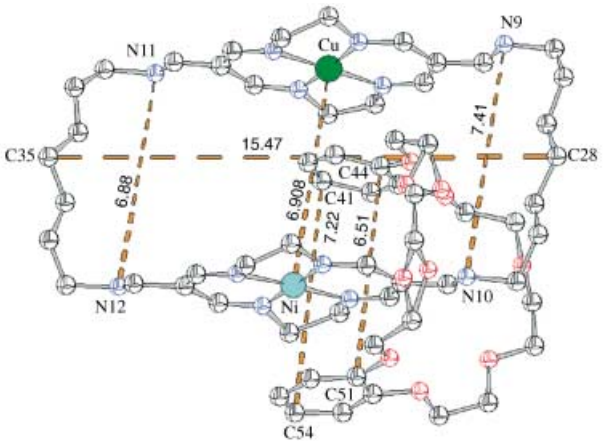


***Figure 1.*** Conformation of **4CuNi** cation with atomic displacement parameters (ADPs) at the 50% probability level. H atoms omitted for clarity.

aromatic rings is located between the two metal-coordinated macrocyclic rings. The second aromatic ring is located almost parallel to the previous one outside the two linked macrocycles. Thus, the one aromatic ring of the crown ether is interlocked between the two macrocycles, and one of the macrocyclic rings is positioned between the two aromatic rings of the crown ether. One of the crown polyether linkers is disordered (see Figure 1), as are the solvent molecules and counterions (see CIF for details). The macrocyclic fragments with aminomethylidyne ends are linked with each other by aliphatic chains that consist of seven carbon atoms each. Therefore, the linked azamacrocyclic fragment of **4CuNi** forms a rectangular cavity with dimensions of 6.91 Å (Cu···Ni) × 15.47 (C28···C35) Å. The metal–metal distance is the shortest of the all three catenanes[23] (dicopper, dinickel, and **4CuNi**). The azamacrocyclic rings are evidently interacting through the guest aromatic ring because the distance between the metal ions is shorter than the distances between exocyclic carbon atoms (Figure 1).

Electrochemical characteristics (peak potentials, $E_{pa}$ and $E_{pc}$, and formal potentials, $E^{o\prime}_{cv}$) of **3CuNi** and **4CuNi** are given in Table 1. For the catenane, the $Ni^{II} \rightarrow Ni^{III}$ oxidation peak

***Table 1:*** Redox characteristics of the compounds studied.[a]

| Compound | $E_{pa}$ [V] | | $E_{pc}$ [V] | | $E^{o\prime}_{cv}$ [V] | $E^{o\prime}_{cv}$ [V] |
|---|---|---|---|---|---|---|
| | $Cu^{II} \rightarrow Cu^{III}$ | $Ni^{II} \rightarrow Ni^{III}$ | $Cu^{III} \rightarrow Cu^{II}$ | $Ni^{III} \rightarrow Ni^{II}$ | $Cu^{II}/Cu^{III}$ | $Ni^{II}/Ni^{III}$ |
| **3NiCu** | 1.081 | 1.351 | 1.008 | 1.281 | 1.045 | 1.316 |
| **4NiCu** | 1.077 | 1.389 | 0.998 | 1.285 | 1.038 | 1.337 |

[a] $E_{pa}$ and $E_{pc}$ are the anodic and cathodic peak potentials $E^{o\prime}_{cv}$

appears at a more positive potential and the reduction of $Cu^{III} \rightarrow Cu^{II}$ at a more negative potential than in the corresponding bismacrocycle. The peaks are lower as the diffusion coefficient of the larger catenane should be smaller than that of the simple bis-macrocycle, but they are also wider, thus reflecting some complications in the electrode process compared to that of the bis-macrocycle. The noted differences are not dependent on the concentration of the electroactive species and, therefore, cannot be attributed to any higher-order chemical reactions or adsorption effects. These features result from the promoting effect of the crown activated by the $d^8$–$d^8$ structure. As described previously, for the simple bis-macrocycle, no intramolecular interactions are observed, since the spacer separating the metal centers (7 $CH_2$ units) is too long. Only for shorter linkers (3 $CH_2$ and 5 $CH_2$ units) could these interactions be detected.[27]

All electrochemical techniques, perhaps most clearly the Osteryoung square-wave (OSW) voltammetry, revealed a very interesting feature of these curves: a splitting of Ni oxidation signals in the case of the catenane system (Figure 2 and Supporting Information). The peak at +1.65 V corresponds to the oxidation of the crown moiety in the catenane. The extent of splitting of the Ni oxidation peaks at about 1.35 V is not a function of the concentration of the catenane

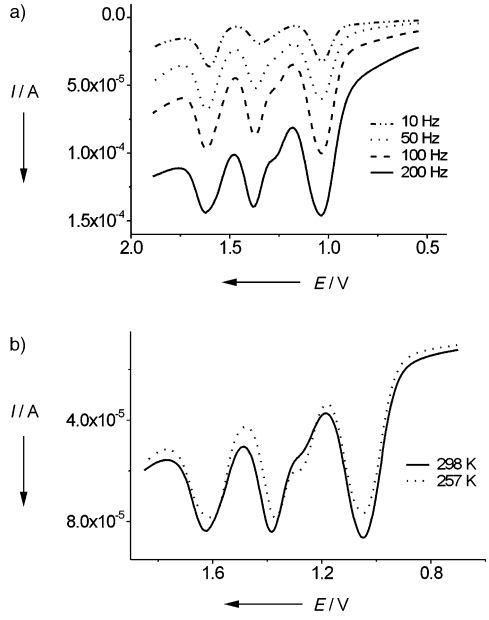


***Figure 2.*** a) OSW voltammograms of 1 mM **4CuNi** in 0.1 M TBAHFP/$CH_3CN$ recorded on a glassy carbon electrode (GCE), $\tilde{\nu}$ = 10 Hz, $\tilde{\nu}$ = 50 Hz, $\tilde{\nu}$ = 100 Hz, $\tilde{\nu}$ = 200 Hz; b) OSW voltammograms of 1 mM **4CuNi** in 0.1 M TBAHFP/$CH_3CN$ recorded on a GCE, $\tilde{\nu}$ = 100 Hz at 298 and 257 K.

 © 2004 Wiley-VCH Verlag GmbH & Co. KGaA, Weinheim 

but is a function of time and temperature. Such behaviour may be understood by assuming that the two different $Ni^{II}$ centers (i.e., they have different local microenvironments) have different populations, even though this happens within the same molecule (Scheme 2).

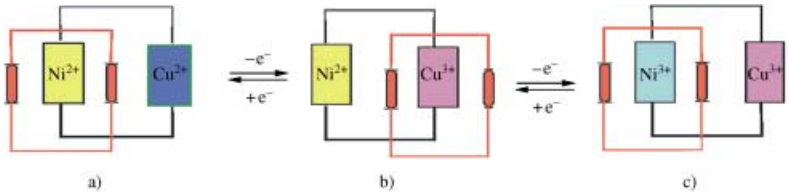


***Scheme 2.*** Schematic representation of electrochemically controlled intramolecular motion.

The donor properties of the first group of $Ni^{II}$ centers is affected by the vicinity of the electron-rich crown ether (Scheme 2a) while the other group is not (Scheme 2b). At lower frequencies (Figure 2a), upon oxidation of $Cu^{II}$ to $Cu^{III}$, the crown-ether unit has enough time to relocate from its initial position close to the $Ni^{II}$ center (Scheme 2a) towards the more positively charged $Cu^{III}$ center (Scheme 2b). As a result of this relocation, the $Ni^{II}$ to $Ni^{III}$ oxidation process appears at more positive potential, since it is free from the influence of the π-electron rich crown ether. However, when the timescale is decreased or the temperature is lowered, the movement of the crown-ether unit is too slow and, in a fraction of the molecules, the $Ni^{II}$ cations remain weakly interacting with the crown ether, thus giving rise to the splitting of peaks. Hence, the decrease of temperature (Figure 2b) leads to an increase in the development of the negative peak corresponding to the oxidation of nickel centers still surrounded by the crown ether. Therefore, the "frozen" interconversion within the molecule can be clearly shown at lower temperatures at which the movement of the crown ether unit is slowed down. The most remarkable feature of this new catenane is that each electrochemical step triggers a rearrangement of the compound (Scheme 2). The intramolecular movement upon the application of appropriate potential is clearly seen in the normal-pulse (NP) voltammetry experiment with different initial potentials (Figure 3).

In this experiment, the potential between the pulse application, $E_i$, is set at a chosen value for 2 seconds and then 50 ms pulses of increasing amplitude are applied to the electrode. When $E_i$ is set to 0.7 V, no redox reaction can proceed in these two seconds, and only during the pulse application can some movement of the crown towards $Cu^{III}$ center be triggered. A part of the $Ni^{II}$ centers is then freed from the crown influence. The formation of these two different populations of the Ni centers results in the splitting of waves, which is easier to distinguish when the curves are differentiated (Figure 3a and Table 2). By varying the pulse time, we can obtain the time constant of the observed motion based on the ratio of oxidation wave currents, which is about 5.3 $s^{-1}$.

At 1.15 V, $Cu^{III}$ is generated in the vicinity of the electrode during the 2 s at $E_i$ and induces a swing of the crown unit towards the oxidized copper center (Scheme 2, position b, Table 2). As shown in Figure 3c, the more positive $Ni^{II}$ oxidation peak (Ni center freed from the influence of the

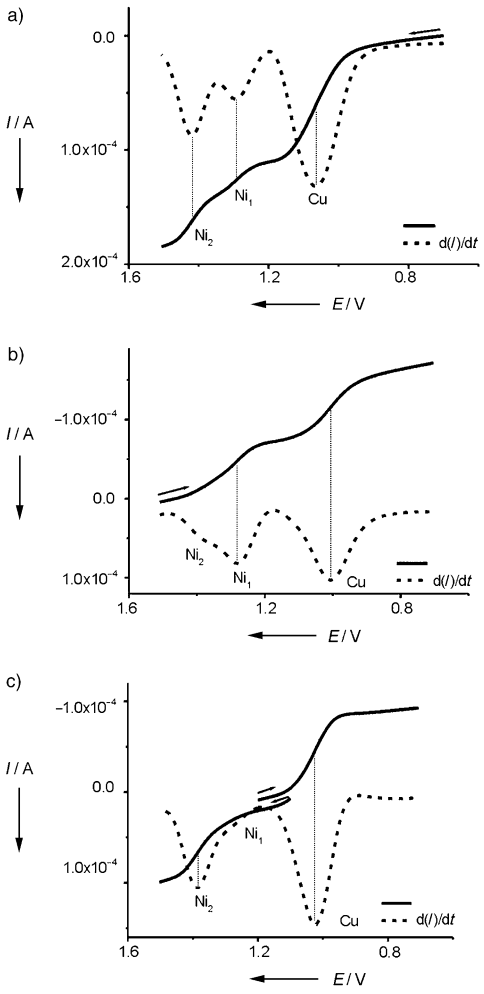


***Figure 3.*** NP voltammograms and their derivatives for 1 mM **4CuNi** in 0.1 M TBAHFP/$CH_3CN$ recorded on a GCE, $t_P = 50$ ms, $t_w = 2$ s. $E_i$: a) 0.70, b) 1.50, c) 1.15 V.

***Table 2:*** The dependence of half-wave potentials of the NP waves on the potential applied to the electrode between the application of pulses ($E_i$).[a]

| $E_i$, direction of pulses | Metal center | $E_{1/2}$ [V] | $E_{1/2}$ [V][b] |
|---|---|---|---|
| 0.7 V | Cu | 1.062 | 1.063 |
| | $Ni_1$ | [c] | 1.291 |
| 0.7→1.5 | $Ni_2$ | 1.430 | 1.419 |
| 1.15 V | Cu | 1.024 | 1.024 |
| 1.15→0.7 | | | |
| 1.15 V | $Ni_1$ | [c] | [c] |
| 1.15→1.5 | $Ni_2$ | 1.374 | 1.387 |
| 1.5 V | Cu | 1.007 | 1.006 |
| | $Ni_1$ | 1.303 | 1.280 |
| 1.5→0.7 | $Ni_2$ | [c] | [c] |

[a] **4CuNi** [1 mM] in TBAHFP/$CH_3CN$ [0.1 M]; pulse time $t_P = 50$ ms, time window between pulses $t_w = 2$ s. [b] Based on the derivatized NP curves. $E_i$: potential during 2 s ($t_w$) between application of pulses. [c] Signal poorly resolved, $E_{1/2}$ potential difficult to determine.

 © 2004 Wiley-VCH Verlag GmbH & Co. KGaA, Weinheim 

crown ether) clearly dominates in the voltammogram. On the other hand, when $E_i$ is set to 1.5 V, both $Ni^{III}$ and $Cu^{III}$ centers are generated during the time between the application of pulses. The crown ether is located close to the nickel center again and the $Ni^{II}/Ni^{III}$ peak reappears at more negative potential (Scheme 2c). The position of the $Cu^{III}$ reduction signal depends on the length of the pulses. When longer pulses are applied, the concentration of reduced $Ni^{II}$ ions is higher at the time when the current for $Cu^{III}$ reduction is probed. Hence the fraction of molecules with the crown ether relocated towards the Cu center is larger. These electrochemically switched relocations reflect a shuttlelike behavior triggered by the application of an appropriate potential. We would like to point out here the unique ability of the Osteryoung square-wave and reverse-pulse techniques to detect intramolecular motion triggered by applied potential.

To our knowledge, this is the first example of the synthesis of a transition-metal heterodinuclear catenane that reveals translocation of the crown unit back and forth between two different metal centers in response to an external stimulus—an applied potential. By applying appropriate potentials either copper or nickel centers (or both) are reversibly oxidized to the higher (+3) oxidation state, which favors an interaction of these centers with the π-electron-rich aromatic system of the crown unit resulting in the relocation of the crown towards the oxidized metal center. The nickel centers affected by the catechol groups are oxidized more easily than those that are not surrounded by the crown units. This "frozen" interconversion within the molecule can be better observed at lower temperature or shorter time scales. The phenomenon of controlled intramolecular motion can potentially be applied in molecular devices.

## Experimental Section

The solvents and reagents used in these studies were reagent grade or better. Acetonitrile was dried over $P_2O_5$ and distilled under argon. 6,13-Bis(metoxymethylidene)-1,4,8,11-tetrazacyclotetradeca-4,7,11,14-tetraenenickel(II) hexafluorophosphate (**1Ni**) and 6,13-bis(7′-ammoniumheptaneaminomethylidene)-1,4,8,11-tetrazacyclotetradeca-4,7,11,14-tetraene copper(II) hexafluorophosphate (**2Cu**) were synthesized according to the previously published procedures.[23,27]

Preparation of **3CuNi** and **4CuNi**: Dibenzo-24-crown-8 (0.75 g, 1,7 mmol), copper **2Cu** (0.50 g, 0,45 mmol) and nickel **1Ni** macrocyclic complexes (0,285 g, 0.45 mmol) were dissolved in 100 $cm^3$ of dry acetonitrile that contained $Et(iPr)_2N$ (0.2 $cm^3$) and stirred at room temperature. After 4 h the solvent was removed by rotary evaporation to give a dark-orange oil. The oil was then dissolved in dichloromethane absorbed on the top of a 2 × 25 cm neutral $Al_2O_3$ column. The column was washed with chloroform until all excessive crown ether had been collected. An orange band that remained on the top of column was then eluted with an acetonitrile solution that contained $NH_4PF_6$ (1 g/100 mL). The collected orange eluate was concentrated, diluted with water and absorbed on a SP Sephadex C-25 column. The column was washed with a small amount of water/acetonitrile (1:1), then with water, and finally eluted with 0.5 M NaCl solution. Two orange bands were collected and products precipitated upon addition of $NH_4PF_6$. The precipitates were removed by filtration, dissolved in acetonitrille that contained small amount of $NH_4PF_6$ and diluted with ethanol and water. Products precipitated upon slow evaporation of solvents were isolated by filtration and washed with ethanol. The first fraction contained the catenane **4CuNi** (0.095 g, 12%) and the second the previously described bismacrocyclic complex **3CuNi**[27] (0.200 g, 33%).

**4CuNi**: $C_{62}H_{92}O_8N_{12}CuNi\cdot(PF_6)_4\cdot 2H_2O$ (1835.6): Elemental analysis (%) calcd C 39.8, H 5.1, N 9.0; found: C 40.1, H 5.3, N 9.0; IR (nujol): $\tilde{\nu}$ = 3370, 1660, 1621vs, 1590, 846vs, 559 $cm^{-1}$; ESI MS(*m*/*z*): 313.9 $[C_{62}H_{92}O_8N_{12}CuNi]^{4+}$, 466.8 $[C_{62}H_{92}O_8N_{12}CuNi\cdot(PF_6)]^{3+}$, 772.4 $[C_{62}H_{92}O_8N_{12}CuNi\cdot(PF_6)_2]^{2+}$.

Voltammetry*:* Linear scan, normal-pulse-and square-wave voltammetry experiments were performed by using the Autolab potentiostat (ECO Chemie, Netherlands) in three electrode arrangement with a silver/silver chloride (Ag/AgCl) as the reference, platinum foil as the counter and glassy carbon electrode (GCE, BAS, 3 mm diameter) as the working electrode. The reference electrode was separated from the working solution by an electrolytic bridge filled with 0.1 M tetrabutylammonium hexafluorphosphate (TBAHFP)/$CH_3CN$ solution. The reference-electrode potential was calibrated by using ferrocene oxidation in the same TBAHFP/$CH_3CN$ solution. The acetonitrile containing 0.1 M TBAHFP was used as the supporting electrolyte solution. Argon was used to de-aerate the solution and an argon atmosphere was maintained over the solution during the experiments.

Supporting Information available: ESI mass spectra, cyclic and OSW voltammograms for **4CuNi**.

Received: July 31, 2003
Revised: January 1, 2004 [Z52528]

**Keywords:** catenanes · electrochemistry · macrocyclic ligands · molecular devices · pi interactions

[1] a) P. L. Anelli, P. R. Ashton, R. Ballardini, V. Balzani, M. Delgado, M. T. Gandolfi, T. T. Goodnow, A. E. Kaifer, D. Philip, M. Pietraszkiewicz, L. Prodi, M. V. Reddington, A. M. Z. Slawin, N. Spencer, J. F. Stoddart, C. Vincent, D. J. Williams, *J. Am. Chem. Soc.* **1992**, *114*, 193–218; b) "Molecular Machines and Motors": L. Raehm, J. P. Sauvage, *Struct. Bonding (Berlin)* **2001**, *99*, 55; c) J. F. Stoddart, *Acc. Chem. Res.* **2001**, *34*, 410–411; d) V. Amendola, L. Fabbrizzi, C. Mangano, P. Pallavicini, *Acc. Chem. Res.* **2001**, *34*, 488–493.

[2] A. E. Kaifer, *Acc. Chem. Res.* **1999**, *32*, 62–71.

[3] C. Bird, A. T. Kuhn, *Chem. Soc. Rev.* **1981**, *10*, 49–82.

[4] A. Mirzoian, A. E. Kaifer, *Chem. Eur. J.* **1997**, *3*, 1052–1058.

[5] P. R. Ashton, T. T. Goodnow, A. E. Kaifer, M. V. Reddington, A. M. Z. Slawin, N. Spencer, J. F. Stoddart, *Angew. Chem.* **1989**, *101*, 1404–1408; *Angew. Chem. Int. Ed. Engl.* **1989**, *28*, 1396–1399.

[6] A. R. Bernardo, J. F. Stoddart, A. E. Kaifer, *J. Am. Chem. Soc.* **1992**, *114*, 10624–10631.

[7] P. R. Ashton, D. Philip, N. Spencer, J. F. Stoddart, D. J. Williams, *J. Chem. Soc. Chem. Commun.* **1994**, 181–182.

[8] W. Devonport, M. A. Blower, M. R. Bryce, L. M. Goldenberg, *J. Org. Chem.* **1997**, *62*, 885–887.

[9] J.-C. Chambron, J.-P. Sauvage, K. Mislow, A. De Cian, J. Fischer, *Chem. Eur. J.* **2001**, *7*, 4085–4096.

[10] D. J. Cardenas, P. Gavina, J.-P. Sauvage, *J. Am. Chem. Soc.* **1997**, *119*, 2656–2664.

[11] R. A. Bissel, E. Cordova, A. E. Kaifer, *J. Org. Chem.* **1995**, *60*, 1033–1038.

[12] M. Asakawa, P. R. Ashton, R. Ballardini, V. Balzani, A. Credi, C. Harmes, G. Mattersteig, M. Montalti, A. N. Shipway, N. Spencer, J. F. Stoddart, M. S. Tolley, M. Venturi, A. J. P. White, D. J. Williams, *Angew. Chem.* **1998**, *110*, 357–361; *Angew. Chem. Int. Ed.* **1998**, *37*, 333–337.

[13] P. R. Ashton, R. Ballardini, V. Balzani, M. Belohradsky, M. T. Gandolfi, D. Phillip, L. Prodi, F. M. Raymo, M. V. Reddington,

 © 2004 Wiley-VCH Verlag GmbH & Co. KGaA, Weinheim 

N. Spencer, J. F. Stoddart, M. Venturi, D. J. Williams, *J. Am. Chem. Soc.* **1996**, *118*, 4931 – 4951.
[14] C. P. Collier, G. Mattersteig, E. W. Wong, Y. Luo, K. Beverly, J. Sampaio, F. M. Raymo, J. F. Stoddart, J. R. Heath, *Science* **2000**, *289*, 1172 – 1175.
[15] A. M. Brouwer, C. Frochot, F. G. Gatti, D. A. Leigh, L. Mottier, F. Paolucci, S. Roffia, G. W. H. Wurpel, *Science* **2001**, *291*, 2124 – 2128.
[16] D. B. Amabilino, P. L. Anelli, P. R. Ashton, G. R. Brown, E. Cordova, L. A. Godinez, W. Hayes, A. E. Kaifer, D. Philip, A. M. Z. Slawin, N. Spencer, J. F. Stoddart, M. S. Tolley, D. J. Williams, *J. Am. Chem. Soc.* **1995**, *117*, 11142 – 11170.
[17] P. R. Ashton, C. L. Brown, J. Cao, J.-Y. Lee, S. P. Newton, F. M. Raymo, J. F. Stoddart, A. J. P. White, D. J. Williams, *Eur. J. Org. Chem.* **2001**, 957 – 965.
[18] M. Perez-Alvarez, F. M. Ryamo, S. J. Rowan, D. Schiraldi, J. F. Stoddart, Z.-H. Wang, A. J. P. White, D. J. Williams, *Tetrahedron* **2001**, *57*, 3799 – 3808.
[19] P. R. Ashton, R. Ballardini, V. Balzani, M. T. Gandolfi, D. J.-F. Marquis, L. Perez-Garcia, L. Prodi, J. F. Stoddart, M. Venturi, *J. Chem. Soc. Chem. Commun.* **1994**, 177 – 178.
[20] V. Balzani, A. Credi, S. J. Langford, F. M. Ryamo, J. F. Stoddart, M. Venturi, *J. Am. Chem. Soc.* **2000**, *122*, 3542 – 3543.
[21] P. R. Ashton, S. E. Boyd, A. Brindle, S. J. Langford, S. Menzer, L. Perez-Garcia, J. A. Preece, F. M. Ryamo, N. Spencer, J. F. Stoddart, A. J. P. White, D. J. Williams, *New J. Chem.* **1999**, *23*, 587 – 602.
[22] A. Livoreil, C. O. Dietrich-Buchecker, J.-P. Sauvage, *J. Am. Chem. Soc.* **1994**, *116*, 9399 – 9400.
[23] B. Korybut-Daszkiewicz, A. Więckowska, R. Bilewicz, S. Domagała, K. Woźniak, *J. Am. Chem. Soc.* **2001**, *123*, 9356 – 9366.
[24] R. A. Bissell, E. Cordova, A. E. Kaifer, J. F. Stoddart, *Nature* **1994**, *369*, 133 – 137.
[25] P. A. Ashton, P. Ballardini, V. Balzani, A. Credi, M. T. Gandolfi, S. Menzer, L. Perez-Garcia, L. Prodi, J. F. Stoddart, M. Venturi, A. J. P. White, D. J. Williams, *J. Am. Chem. Soc.* **1995**, *117*, 11171 – 11197.
[26] A. Livoreil, J.-P. Sauvage, N. Amaroli, V. Balzani, L. Flamingni, B. Ventura, *J. Am. Chem. Soc.* **1997**, *119*, 12114 – 12124.
[27] A. Więckowska, R. Bilewicz, S. Domagała, K. Woźniak, B. Korybut-Daszkiewicz, A. Tomkiewicz, J. Mroziński, *Inorg. Chem.* **2003**, *42*, 5513 – 5522.
[28] **4CuNi**: $CuNiC_{66}N_{14}H_{100}P_4F_{24}O_9$, $M_r = 1935.73$; $T = 100$ K; $\lambda = 0.71073$ Å; triclinic; space group $P\bar{1}$; unit cell dimensions: $a = 15.495(3)$ Å, $b = 16.886(3)$ Å, $c = 16.969(3)$ Å, $\alpha = 80.25(3)°$, $\beta = 89.47(3)°$, $\gamma = 81.74(3)°$; $V = 4330(2)$ Å$^3$; $Z = 2$; $\rho$ (calcd) = 1.485 Mg m$^{-3}$; absorption coefficient = 0.647 mm$^{-1}$; $F(000) = 1998$; crystal size = $0.5 \times 0.4 \times 0.2$ mm$^3$; $\theta$ range for data collection = 3.23–22.00°; index ranges: $-16 \le h \le 16$, $-17 \le k \le 17$, $-17 \le l \le 17$; reflections collected = 49711; independent reflection = 10582 [$R_{int} = 0.0612$]; refinement method, full-matrix least-squares on $F^2$; data/restraints/parameters = 10582/35/1161; goodness-of-fit on $F^2 = 1.113$; final R indices [$I > 2\sigma(I)$]: $R1 = 0.0899$, $wR2 = 0.2487$; $R$ indices (all data): $R1 = 0.1084$, $wR2 = 0.2704$; extinction coefficient = 0; weight = $1/[\sigma^2(F_o^2) + (0.1687P)^2 + 7.3416P]$ where $P = (\mathrm{Max}(F_o^2, 0) + 2F_c^2)/3$; largest diffraction peak and hole = 1.282 and −0.892 e Å$^{-3}$. CCDC 214048 (**4CuNi**) contains the supplementary crystallographic data for this paper (excluding structure factors). These data can be obtained free of charge via www.ccdc.cam.ac.uk/conts/retrieving.html (or from the Cambridge Crystallographic Data Centre, 12 Union Road, Cambridge CB2 1EZ, UK; fax: (+44) 1223-336-033; or deposit@ccdc.cam.ac.uk).

 © 2004 Wiley-VCH Verlag GmbH & Co. KGaA, Weinheim 